

Article

A Prediction Model of Pressure Loss of Cement Slurry in Deep-Water HTHP Directional Wells

Kunhong Lv ¹, Hao Huang ^{1,*}, Xingqiang Zhong ², Yian Tong ³, Xingjie Ling ¹ and Qiao Deng ^{1,*}

¹ College of Petroleum Engineering, Yangtze University, Wuhan 430199, China; lkhyxr@163.com (K.L.); lingxingjie2000@163.com (X.L.)

² Zhanjiang Operation Company, CNOOC Petrochemicals Division, Zhanjiang 524000, China; zhongxingqiang168@163.com

³ Downhole Service Company, CNPC Chuanqing Drilling Engineering Co., Ltd., Chengdu 610052, China; tongzgsy@163.com

* Correspondence: 18772645696@163.com (H.H.); dengqiao@yangtzeu.edu.cn (Q.D.)

Abstract: The exploitations of deep-water wells often use directional well drilling to reach the target layer. Affected by special environments in deep water, the prediction of pressure loss of cement slurry is particularly important. This paper presents a prediction model of pressure loss suitable for deep-water directional wells. This model takes the complex interaction between the temperature, pressure and hydration kinetics of cement slurry into account. Based on the initial and boundary conditions, the finite difference method is used to discretize and calculate the model to ensure the stability and convergence of the result calculated by this model. Finally, the calculation equation of the model is used to predict the transient temperature and pressure loss of Wells X1 and X2, and a comparison is made between the predicted value and the monitoring data. The comparison results show that the maximum error between the temperature and pressure predicted by the model and the field measured value is within 6%. Thus, this model is of high accuracy and can meet the needs of site construction. It is concluded that this result can provide reliable theoretical guidance for temperature and pressure prediction, as well as the anti-channeling design of HTHP directional wells.

Keywords: deep water; directional wells; pressure loss; hydration reaction kinetics; temperature and pressure coupling; prediction model



Citation: Lv, K.; Huang, H.; Zhong, X.; Tong, Y.; Ling, X.; Deng, Q. A Prediction Model of Pressure Loss of Cement Slurry in Deep-Water HTHP Directional Wells. *Energies* **2021**, *14*, 8180. <https://doi.org/10.3390/en14238180>

Academic Editors: Reza Rezaee and Riyaz Kharrat

Received: 10 October 2021

Accepted: 2 December 2021

Published: 6 December 2021

Publisher's Note: MDPI stays neutral with regard to jurisdictional claims in published maps and institutional affiliations.



Copyright: © 2021 by the authors. Licensee MDPI, Basel, Switzerland. This article is an open access article distributed under the terms and conditions of the Creative Commons Attribution (CC BY) license (<https://creativecommons.org/licenses/by/4.0/>).

1. Introduction

In recent years, the focus of oil–gas exploration and development has gradually shifted from shallow-water areas to deep-water areas. Compared with land and shallow water cementing, deep-water cementing operations are faced with the difficulties of high temperature, high pressure and special environments, bringing great challenges to oil–gas exploration and development. The annular channeling formed in the cementing stage has also become a problem to be solved urgently in the oil, natural gas and hydrate industries [1,2]. During the waiting on cement stage, with the progression of the hydration reaction, the gas will gradually enter the annulus space and cause gas channeling, which occurs when the liquid column pressure is lower than the formation pressure [3–6]. At present, there are three mainstream views on the causes of annular channeling both at home and abroad. In the cementing process, the residual drilling fluid caused by low displacement efficiency forms a channeling channel. During the waiting on cement stage, a channeling path is formed by formation fluid entering the annular gap when the annular liquid head is lower than the formation pressure due to the weight loss of cement slurry in the waiting on cement (WOC) stage. After cement slurry solidification, a channeling path is formed after the setting of cement slurry because of the poor cementing quality between the cement sheath and borehole wall, as well as the casing. In the above three viewpoints, the weight loss of cement slurry in the WOC stage is the main cause of annular channeling.

Therefore, it is particularly important to carry out research on the prediction of the pressure loss of cement slurry.

In the process of weight loss during the WOC stage, the continuous development of static gelling strength leads to insufficient pressure in the cement slurry column to stabilize the formation, which provides a driving force for the annular air channeling [7,8]. Therefore, the establishment of an accurate temperature and pressure field calculation model and a pressure loss prediction model is a prerequisite for the safe and efficient cementing of high-temperature and high-pressure (HTHP) wells. Regarding this field of research, there have already been some achievements. Carter et al. [9] believed that the bridge blinding caused by the gelatinization and filtration of cement slurry hindered the effective transmission of the upper hydrostatic column pressure, which was an important reason for the weight loss of cement slurry. Sabins et al. [10,11] first found that volume shrinkage and gelatinization led to a decrease in liquid column pressure acting on the bottom of the well, resulting in the weight loss of cement slurry, and then put forward a corresponding theoretical model. Parcevaux et al. [12] proposed a relationship between pressure drop in the cement slurry column and gel strength, then provided a corresponding correlation. Sun [13] studied the pore pressure drops of three types of cement slurry due to settling, settling–gelling (SG) weight loss and hydrated volume shrinking–gelling (HG) weight loss, then further analyzed the relationship between the three without filtration, revealing their internal mechanism and law. Zhang et al. [14–16] studied the important influence of cement slurry's stability on weight loss with a large number of weight loss experiments based on the force analysis of cement slurry in the annulus. They also studied the quantitative relationship between effective slurry column pressure and gas cutting resistance and the factors that affect the former two and set up a calculation model for the process of cement slurry setting, making the condition to cause breakthrough flow in the annulus, which can be used for predicting and evaluating the channeling preventing the ability of cement slurry in the process of setting. Bu et al. [17] established a mechanical model of the weight loss of cement slurry. They concluded that the weight loss of cement slurry is mainly related to the area of the annulus wall and the formation speed of cement slurry. Since the slurry temperature in the annulus varies with depth, the build-up of gel strength and pressure drop are different at different depths, and the hydraulic pressure loss of the slurry column is calculated in sections. Li et al. [18] established an accurate calculation model of hydraulic pressure loss of slurry and a developed sectional design and balanced cementing methods, which provided an effective calculation model for anti-gas channeling cementing design. Cheng et al. [19] investigated the evolution of cement slurry properties during liquid–solid transition by tests using X-ray diffraction (XRD), thermogravimetry (TG) and mechanical analysis and explained the causes of pressure loss in cement slurry from a microscopic point of view. Liu et al. [20] developed an apparatus for evaluating the pressure loss of cement slurry at HTHP conditions by scaling down the sizes of existing apparatus. They carried out typical cement slurry weight loss pressure experiments in vertical wells and inclined wells and proposed a piecewise calculation method of pressure loss, which has been tested in the field.

At present, the research of different scholars on the prediction model of pressure loss is mainly realized by the weight loss method and testing the change in static gelling strength [21,22]. However, affected by the downhole complex environment and self-performance of cement slurry, it is difficult to accurately calculate the actual pressure loss merely based on existing models or experimental tests. In view of this, a model for calculating the pressure loss in the WOC stage was derived in this research, taking into comprehensive consideration the mutual action between the hydration reaction, temperature and pressure of cement slurry, as well as the complicated deep-water environment. Finally, a comparison was made between the result measured on the site of Well X in a block of a field, and the result was calculated on the basis of this model. The comparison result verifies the accuracy and stability of the model, which can provide more safe and effective guidance for cementing construction.

2. Modeling

2.1. Physical Model of Wellbore

Most offshore oil–gas wells are directional wells with wellbore configuration [2]. In the process of cement injection, when cement slurry is displaced to the design depth of the annulus, it marks the completion of the injection and the starting of the WOC stage. For the HTHP well, during this stage, the cement slurry will undergo a violent hydration reaction, with temperature and pressure varying with time and space change. The model area is divided into 3 blocks: formation, cement slurry in annular space and drilling fluid in the casing. The model is axisymmetric about the central axis of the wellbore (Figure 1).

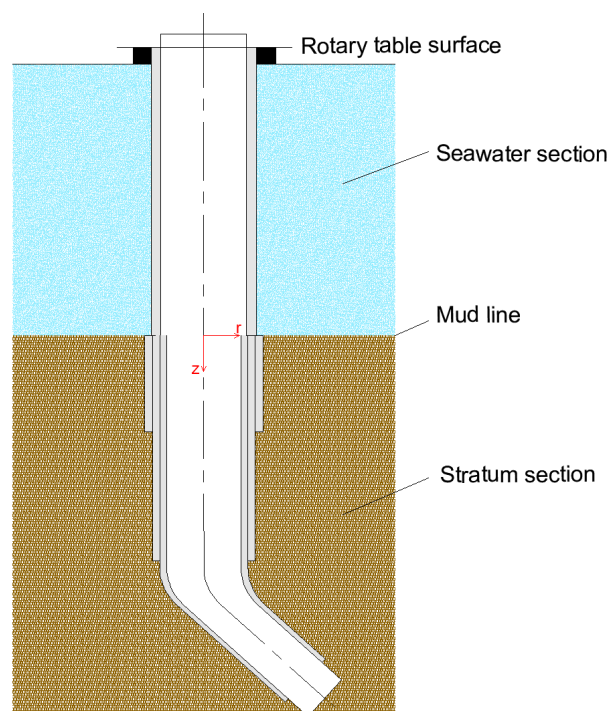


Figure 1. Schematic diagram of the body structure of HTHP directional well.

2.2. Establishment for Wellbore Temperature Field Model

2.2.1. Fundamental Assumptions

When establishing the pressure loss calculation model, for the convenience of the research, the following hypotheses were made for the model:

- Above the formation is a constant-temperature zone, which is homogeneously isotropic with constant physical parameters;
- The calculation satisfies Fourier's law, and the geothermal gradient is known, not considering heat source and fluid thermal convection, but only considering horizontal and vertical heat conduction;
- The heat convection in the wellbore is radial steady-state heat transfer, regardless of the axial temperature difference of the annular fluid;
- The physical parameters (such as density, specific heat capacity, thermal conductivity, etc.) of each material in this model are always constant, which do not change with external factors. The specific heat and thermal conductivity are the same in the vertical and horizontal directions;
- Assuming that the drilling fluid and cement slurry do not mix with each other, they do not react with each other, and the interface is stable.

2.2.2. Model Establishment

During the WOC stage, after the injection displacement of the cement slurry in place, with the heat exchange of the wellbore, the temperature field in the wellbore changes in real time [23,24]. There are three main influencing factors: heat conduction between cement slurry and drilling fluid in the casing, heat conduction between cement slurry and formation and temperature rise of the cement slurry due to hydration heat. A cylindrical coordinate system is plotted along the downward axial direction of the wellbore, with the origin located at the center of the well head. In the axial direction, the wellbore formation is separated into several control units according to the heat transfer medium and the well structure. Then, any micro unit with length Δz is taken as the research object (Figure 2).

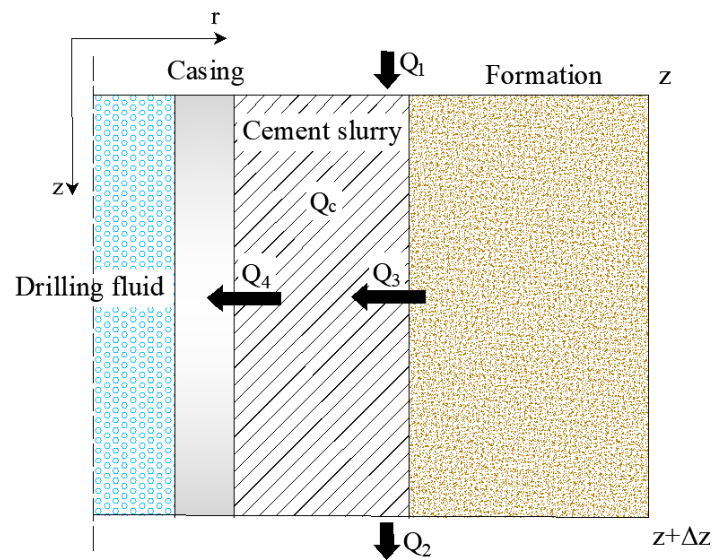


Figure 2. Schematic diagram of energy transfer in wellbore micro unit.

The energy exchange between the micro unit and adjacent micro unit above is expressed as:

$$Q_1 = A_a k_{df} \Delta t \frac{T_{df}|_{z+\Delta z} - T_{df}|_z}{\Delta z} \quad (1)$$

where A_a is the cross-sectional area of the annular space, m^2 ; k_c is the thermal conductivity of cement slurry, $W/(m \cdot K)$; Δt is the time stepping, s ; T_{df} is the temperature of the drilling fluid, K ; and Δz is the length of the micro unit, m .

The energy exchange between the micro unit and adjacent micro unit below is expressed as:

$$Q_2 = A_c k_{df} \Delta t \frac{T_{df}|_z - T_{df}|_{z-\Delta z}}{\Delta z} \quad (2)$$

where A_c is the cross-sectional area of the tubular string, m^2 ; and k_{df} is the thermal conductivity of the drilling fluid, $W/(m \cdot K)$;

The energy exchange between cement slurry and the formation is presented as:

$$Q_3 = 2\pi r_w U_a (T_{e,0} - T_e) \Delta t \Delta z \quad (3)$$

where r_w is the radius of the wellbore, m ; U_a is the overall heat transfer coefficient from the annular space to the formation, $W/(m^2 \cdot K)$; $T_{e,0}$ is the temperature at the interface between the wellbore and formation, K ; and T_e is the temperature of the formation, K .

The energy exchange between the cement slurry and the casing is shown below:

$$Q_4 = 2\pi r_{ci} U_c (T_c - T_{df}) \Delta t \Delta z \quad (4)$$

where r_{ci} is the inner diameter of the casing, m; U_c is the overall heat transfer coefficient from the casing to the annular space, $W/(m^2 \cdot K)$.

The energy gain and loss of the micro unit satisfies the law of conservation of energy. Based on this, the heat conduction model of the formation, the drilling fluid in the casing and the cement slurry in the annulus and the corresponding difference form can be obtained:

The internal of formation: The heat transfer in formation satisfies the heat diffusion equation:

$$\frac{\partial^2 T_e}{\partial z^2} + \frac{\partial^2 T_e}{\partial r^2} + \frac{1}{r} \frac{\partial T_e}{\partial r} = \frac{\rho_e c_e}{k_e} \frac{\partial T_e}{\partial t} \quad (5)$$

where ρ_e is the density of the formation, kg/m^3 ; c_e is the specific heat capacity of formation, $J \cdot kg^{-1} \cdot K^{-1}$; and k_e is heat conductivity of the formation, $W/(m^2 \cdot K)$.

Heat conduction model of drilling fluid in the casing: The energy variation of the micro unit with length Δz comes from the energy exchange of the adjacent micro units above and below it and the heat exchange between the casing and the annular space. The heat conduction model and the corresponding difference form are expressed as follows:

$$\left(T_{df}|_{t+\Delta t} - T_{df}|_t \right) c_f \rho_f A_c \Delta z = 2\pi r_{ci} U_c (T_c - T_{df}) \Delta t \Delta z - A_c k_{df} \Delta t \frac{T_{df}|_z - T_{df}|_{z-\Delta z}}{\Delta z} + A_c k_{df} \Delta t \frac{T_{df}|_{z+\Delta z} - T_{df}|_z}{\Delta z} \quad (6)$$

Heat conduction model of cement slurry in the annular space: The energy change of the micro unit with length Δz was derived from the energy exchange with the adjacent micro units above and below it and the heat exchange between the casing and the annular space, the heat conduction between the annular space and formation and the hydration heat caused by cement slurry itself.

For the HTHP well, hydration heat of cement slurry is also a problem to consider, as it can lead to a temperature rise of the cement slurry and accelerate the hydration rate of cement slurry. The heat released by cement slurry in the annular space can be calculated on the basis of hydration kinetics:

$$Q = (\alpha|_{t+\Delta t} - \alpha) Q_{\max} \rho_c A_a \Delta z \quad (7)$$

According to the law of conservation of energy, and Equations (5)–(7), the heat transfer model of cement slurry in the annular space can be expressed as:

$$\begin{aligned} (T_c|_{t+\Delta t} - T_c|_t) c_c \rho_c A_a \Delta z = & (\alpha|_{t+\Delta t} - \alpha) Q_{\max} \rho_c A_a \Delta z \\ & - 2\pi r_{ci} U_c (T_c - T_f) \Delta t \Delta z + 2\pi r_w U_a (T_{e,0} - T_c) \Delta t \Delta z \\ & - A_a k_c \Delta t \frac{T_c|_z - T_c|_{z-\Delta z}}{\Delta z} + A_a k_c \Delta t \frac{T_c|_{z+\Delta z} - T_c|_z}{\Delta z} \end{aligned} \quad (8)$$

where Q is the hydration heat of cement slurry at any time, J/kg ; α is the degree of hydration of cement slurry; Q_{\max} is the total heat released by hydration of cement slurry, J/kg ; and ρ_c is the density of cement slurry, kg/m^3 .

Rewriting Equation (6) in differential form:

$$\frac{\partial T_f}{\partial t} = \frac{2\pi r_{ci} U_c}{c_f \rho_f A_c} (T_c - T_f) + \frac{k_f}{c_f \rho_f} \frac{\partial^2 T_f}{\partial z^2} \quad (9)$$

Combined with Equation (8), Equation (9) can be expressed as the following difference form:

$$\frac{\partial T_c}{\partial t} = \frac{2\pi r_w U_a}{c_c \rho_c A_a} (T_{e,0} - T_c) - \frac{2\pi r_{ci} U_c}{c_c \rho_c A_a} (T_c - T_f) + \frac{Q_{\infty}}{c_c} \frac{\partial \alpha}{\partial t} + \frac{k_c}{c_c \rho_c} \frac{\partial^2 T_c}{\partial z^2} \quad (10)$$

2.3. Establishment of Prediction Model of Pressure Loss of Cement Slurry

After cement slurry is in place, a spatial grid structure with certain strength is formed with the passage of time. Meanwhile, due to the water loss and volume shrinkage of cement slurry during solidification, the cement slurry column has a downward tendency under the action of its own weight and the pressure of the upper slurry column, forming the overall cementing suspension weight loss effect of cement slurry. With the progress of the hydration reaction, the gel strength of cement slurry increases gradually, and the cementing suspension capacity of the grid structure becomes stronger, sharing partial hydrostatic fluid column pressure. Consequently, a constant reduction was seen in the effective pressure of the cement slurry column [25].

During the solidification of cement slurry, for the selected cement slurry cells in the grid structure, the cement slurry's column pressure is:

$$P_e = \rho_c g \Delta z - \frac{4\tau_s \Delta z}{D_w - D_{co}} \quad (11)$$

where P_e is the cement slurry's column pressure, Pa.

Moore et al. [26] proposed an overall cementing suspension weight loss effect of cement slurry on the basis of the classical shear stress model. For directional well, the forces on the model will change. In this model, the cement slurry unit is subjected to five forces (Figure 3):

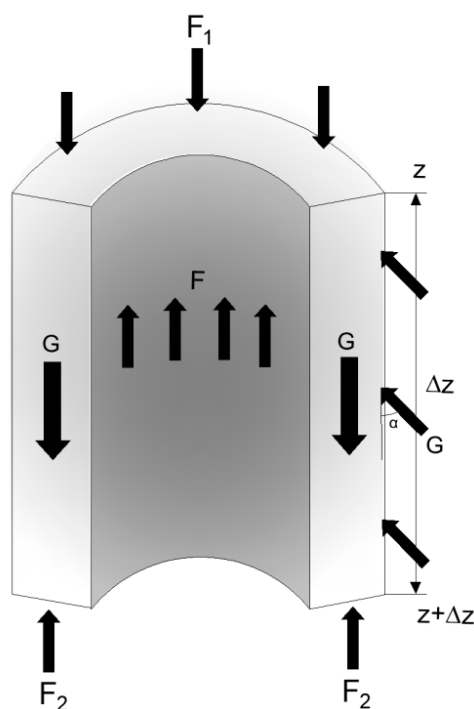


Figure 3. Schematic diagram of forces of the cement slurry micro unit.

The downward force from the upper slurry column:

$$F_1 = \frac{P_1 \times \pi(D_w^2 - D_{co}^2)}{4} \quad (12)$$

The upward force from the lower slurry column:

$$F_2 = \frac{P_2 \times \pi(D_w^2 - D_{co}^2)}{4} \quad (13)$$

Gravity of cell itself:

$$G = \frac{\pi(D_w^2 - D_{co}^2)\gamma\Delta z}{4} \quad (14)$$

where γ is the volumetric weight of cement slurry, M/m^3 ;

Due to the gelling suspension effect, the cement slurry is subjected to the upward cementing suspension force from the shaft wall and the casing:

$$F = \tau_s \times \pi(D_w + D_{co}) \times \Delta z \quad (15)$$

Holding power N perpendicular to the surface of the annular space:

For the cement slurry cell, to meet the force balance, the axial and vertical forces of the cement slurry on the wellbore satisfied the following equation:

$$(G - F_2) \cos \alpha - F_1 - F = 0 \quad (16)$$

$$(G - F_2) \sin \alpha - N = 0 \quad (17)$$

The effective slurry column pressure at the WOC stage of the cement slurry can be obtained as:

$$P_e = \gamma\Delta z \cos \alpha - \frac{4\tau_s\Delta z}{D_w - D_{co}} \quad (18)$$

The corresponding pressure loss could be expressed as:

$$\Delta p = \frac{4\tau_s\Delta z}{D_w - D_{co}} \quad (19)$$

where Δp is the pressure loss, Pa; τ_s is the static gelling strength of cement slurry, Pa; D_w is the diameter of wellbore, m; and D_{co} is the outer diameter of the casing, m.

In the process of cementing, the pressure loss at different depths and moments could be calculated as the following equation:

$$\frac{\partial p}{\partial z} = \max \left\{ \frac{4\tau_s}{D_w - D_{co}}, \rho_w g \right\} \quad (20)$$

where ρ_w is the density of pore water, kg/m^3 .

2.4. Hydration Kinetic Model of Cement Slurry

Hydration kinetics is a method for dynamic research on the hydration reaction based on its internal influence factor (the structure of cement slurry) and external influence factor (the reaction conditions), which can dynamically simulate and depict the hydration process so as to reveal the macro and internal mechanisms of the hydration reaction. For hydration kinetics, the hydration kinetic model of cement-based materials proposed by Krstulović et al. [25] is widely recognized. In this model, the hydration reaction of cement slurry is divided into three processes: nucleation and crystal growth (NG), interactions at the phase boundaries (I) and diffusion (D). The kinetic equations between hydration degree and the reaction time of the three processes and their corresponding differential forms are shown in Equations (21)–(23):

NG Process:

$$\begin{cases} [-\ln(1-\alpha)]^{\frac{1}{n}} = K_{NG}(t-t_0) \\ \frac{d\alpha}{dt} = K_{NG}n(1-\alpha)[- \ln(1-\alpha)]^{\frac{n-1}{n}} \end{cases} \quad (21)$$

I Process:

$$\begin{cases} \left[1 - (1-\alpha)^{\frac{1}{3}}\right]^1 = K_I(t-t_0) \\ \frac{d\alpha}{dt} = 3K_I(1-\alpha)^{\frac{2}{3}} \end{cases} \quad (22)$$

D Process:

$$\begin{cases} \left[1 - (1 - \alpha)^{\frac{1}{3}}\right]^2 = K_D(t - t_0) \\ \frac{d\alpha}{dt} = \frac{3K_D(1-\alpha)^{\frac{2}{3}}}{2\left[1 - (1-\alpha)^{\frac{1}{3}}\right]} \end{cases} \quad (23)$$

where n is the order of chemical reactions; K_{NG} is the reaction rate constant for the process of nucleation and crystal growth, s^{-1} ; K_I is the reaction rate constant for the process of interactions at the phase boundaries, s^{-1} ; K_D is the reaction rate constant for the process of diffusion, s^{-1} ; and t_0 is the terminal stage of the induction period, s.

Isothermal calorimetry can be used to obtain the relationship between the heat release rate dQ/dt , heat release amount Q and time t of the hydration. The hydration degree is usually described by hydration heat and other parameters easy to quantify. The relationship between hydration degree and hydration time is presented as follows:

$$\alpha = Q(t)/Q_{\max} \quad (24)$$

$$\frac{d\alpha}{dt} = \frac{dQ/dt}{Q_{\max}} \quad (25)$$

where t is the hydration reaction time of cement slurry, s; $Q(t)$ is the heat released by the hydration of cement slurry over time, J/kg; and α is the hydration degree of cement slurry.

Chemical reaction rate is significantly affected by temperature. Generally, the hydration rates of cement slurry are higher at higher temperatures. However, for the HTHP well, the wellbore at different depth experiences different temperatures and hydration rates. According to reference [27], the impact of temperature on the chemical reaction rate constant can be expressed by the Arrhenius equation:

$$K = K_0 e^{-E_a/RT} \quad (26)$$

where K is the reaction rate constant, s^{-1} ; K_0 is the prefactor, also called frequency factor, s^{-1} ; E_a is the activation energy of the reactant, $J \cdot mol^{-1}$; R is the ideal gas constant, $J \cdot K^{-1} \cdot mol^{-1}$; and T is the thermodynamic temperature, K.

The progress of the chemical reaction is mainly changed by the impact of temperature field and pressure field on the chemical reaction rate constant. Combined with Equation (9), the relation between chemical reaction rate and temperature and pressure is reflected as follows [28]:

$$K = K_r e^{-E_a/RT} \left[\frac{E_a}{R} \left(\frac{1}{T_r} - \frac{1}{T} \right) + \frac{\Delta V}{R} \left(\frac{p_r}{T_r} - \frac{p}{T} \right) \right] \quad (27)$$

where K_r is the chemical reaction rate constant at the reference temperature and pressure, s^{-1} ; T_r is the reference temperature of the chemical reaction, K; T is the temperature of the chemical reaction, K; p_r is the reference pressure of the chemical reaction, Pa; and p is the pore pressure of cement slurry, Pa.

3. Calculation of the Model

In the cementing process of the HTHP well, the hydration heat has a large influence on the temperature and pressure, and there is also a mutual influence between the temperature and pressure. Therefore, when studying the pressure loss in the WOC stage, the temperature field, pressure field and the hydration kinetic model of cement slurry are coupled by the finite difference method to calculate the model.

3.1. Initial and Boundary Conditions

The following initial and boundary conditions are provided for calculation of the model established in this paper:

1. Initial conditions:

Before the initial hydration, the cement slurry enters the annular space between the casing and the wellbore. The initial condition of the waiting cement slurry is the temperature of the cement slurry at the end of the injection displacement cycle, which is calculated by using the circulating temperature prediction model stated in References [29,30]:

$$\frac{1}{v_f} \frac{\partial T_f}{\partial t} + \frac{\partial T_f}{\partial z} = \frac{2\pi r_{ci} U_c}{c_f w_f} (T_c - T_f) \quad (28)$$

$$\frac{1}{v_c} \frac{\partial T_c}{\partial t} - \frac{\partial T_c}{\partial z} = \frac{2\pi r_w U_c}{c_c w_c} (T_{e,0} - T_c) - \frac{2\pi r_{ci} U_c}{c_c w_c} (T_c - T_f) \quad (29)$$

where $w_f = A_c v_f \rho_f$ is the mass flow rate of drilling fluid in the casing, kg/s; w_c is the mass flow rate of cement slurry in the annular space, kg/s; A_c is the cross-sectional area of casing, m²; and v_f is the circulating velocity of drilling fluid in casing, m/s.

The temperature of the constant-temperature layer is known. As the depth increases, the ground temperature increases linearly in depth and can be calculated on the basis of the geothermal gradient:

$$T_e(r \rightarrow \infty, z, t) = z g_e \cos \theta + T_{const} \quad (30)$$

where g_f is the geothermal gradient, °C/100 m; θ is the deviation angle, °; and T_{cont} is the land surface temperature, °C.

The initial hydration degree of cement slurry is zero:

$$\alpha|_{t=0} = 0 \quad (31)$$

According to the hydrostatic fluid column pressure of cement slurry, the initial pressure of cement slurry can be calculated:

$$p(z)|_{t=0} = \rho_c g z \quad (32)$$

2. Boundary conditions:

Infinitely away from the borehole, the formation temperature is the original static temperature of the formation:

$$\left. \frac{\partial T_e(r, z, t)}{\partial r} \right|_{r \rightarrow \infty} = 0 \quad (33)$$

Because of the axisymmetric calculational domain, the borehole center satisfies the adiabatic condition:

$$\left. \frac{\partial T}{\partial r} \right|_{r=0} = 0 \quad (34)$$

The annular temperature and casing temperature in the bottom of the well are identical:

$$T_c(z = H, t) = T_f(z = H, t) \quad (35)$$

The pore pressure of cement slurry at the wellhead position is environmental pressure:

$$p_0 = p_{en} \quad (36)$$

The formation temperature is the undisturbed ground temperature at a certain distance below the well bottom:

$$T_e(r, z_d + z', t) = T_{const} + t_g(z_d + z') \quad (37)$$

The heat transfer at the wellbore-formation interface can be expressed as:

$$\frac{\partial T_b}{\partial t} \rho_e c_e = \frac{T_c - T_b}{r_w} U_a + \frac{\partial T_b}{r \partial r} k_e \quad (38)$$

where T_b is the wellbore-formation interface temperature, °C.

3.2. Grid Division

Considering that the borehole diameter is much smaller than the length of the wellbore, the model is designed axisymmetric to the center axis of the wellbore in the direction of the borehole diameter.

3.3. Discrete Calculation of the Model

In the process of calculating the model, considering the coupling effect of various factors, the above partial differential equations are transformed into finite difference form by using the finite difference technology of the grid unit on the basis of the above-calculated grid unit in order to improve the calculation accuracy and efficiency:

$$T_{c,i}^{(m+1)} = T_{c,i}^{(m)} - \frac{2\pi r_{ci} U_c \Delta t}{c_c \rho_c A_a} [T_{c,i}^{(m)} = T_{f,i}^{(m)}] + \frac{2\pi r_{wi} U_a \Delta t}{c_c \rho_c A_a} [T_{i,0}^{(m)} = T_{c,i}^{(m)}] + \frac{Q_\infty}{c_c} [\alpha_i^{(m+1)} - \alpha_i^{(m)}] + \frac{k_c \Delta t}{c_c \rho_c} \frac{T_{c,i+1}^{(m)} - 2T_{c,i}^{(m)} + T_{c,i-1}^{(m)}}{\Delta z^2} \quad (39)$$

$$p_i^{(m+1)} = p_{i-1}^{(m+1)} + \max \left\{ \frac{4\tau_s \Delta z}{D_w - D_{co}}, \rho_w g \Delta z \right\} \quad (40)$$

$$\alpha_i^{(m+1)} = \alpha_i^{(m)} + K_{NG} n [1 - \alpha_i^{(m)}] \left\{ -\ln [1 - \alpha_i^{(m)}] \right\}^{\frac{n-1}{n}} \Delta t \quad (41)$$

$$\alpha_i^{(m+1)} = \alpha_i^{(m)} + 3K_1 [1 - \alpha_i^{(m)}] \Delta t \quad (42)$$

$$\alpha_i^{(m+1)} = \alpha_i^{(m)} + \frac{3}{2} \frac{K_D [1 - \alpha_i^{(m)}]^{\frac{2}{3}}}{\left\{ 1 - [1 - \alpha_i^{(m)}]^{\frac{1}{3}} \right\}} \Delta t \quad (43)$$

where M is the last node in the horizontal direction; N is the node at the position at the bottom of the well; n is the order of chemical reactions; m is the time node; i is the space node in the vertical direction; and j is the space node in the horizontal direction.

3.4. Coupling Solution Method

In order to obtain the wellbore temperature and pressure of the HTHP directional well, it is necessary to use the iterative method for calculation. The concrete solving method is as follows: input basic parameters, initial conditions and boundary conditions; mesh radially and axially (Figure 4) and define initial nodes and step sizes; according to the current initial conditions, the temperature, pressure and hydration dynamics parameters at node i are calculated and updated; according to the hydration kinetics model, the hydration kinetics parameters of cement slurry at node i are calculated; combined with the established temperature field model, the transient temperature of node i is calculated; combined with the established pressure field model, the transient pressure of node i is calculated; the temperature and pressure calculation results are checked as per the test data to see whether they reach the required accuracy or not. If not, the calculation should be restarted from Step (3); if yes, the calculation is ended, and the calculation of the next time node is started; output the result.

In order to clearly express the coupled iterative calculation process, a calculation flowchart is drawn (Figure 5).

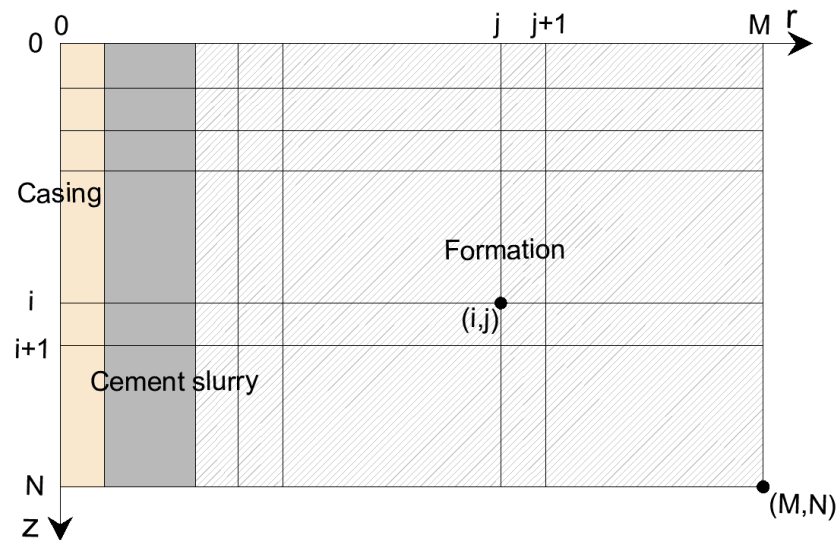


Figure 4. Schematic diagram of grid division.

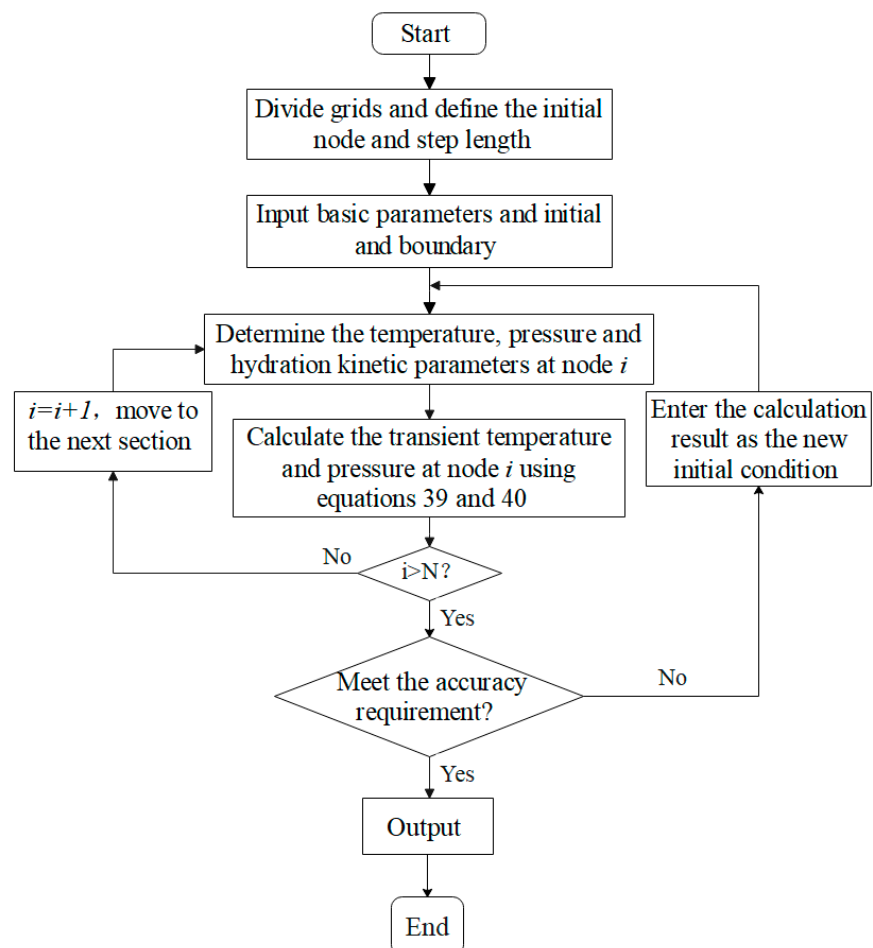


Figure 5. Calculation flowchart of the pressure loss prediction model.

4. Case Analysis

There is a block with 90 m in water depth, 4000–4200 m in buried depth of the reservoir, about 2.30 in pressure coefficient of the reservoir and 195–215 °C in the reservoir temperature, belonging to a typical HTHP gas field. In order to verify the reliability of the model established in this research, a case analysis was carried out on Wells X1 and X2

in this block. The basic parameters and physical parameters of this well are illustrated in Tables 1 and 2.

Table 1. Basic parameters of Well X1.

Parameter	Value	Parameter	Value
Well type	Directional well	Thermal conductivity of formation ($\text{W}\cdot\text{m}^{-1}\cdot\text{K}^{-1}$)	2.03
Well depth (m)	5150	Thermal conductivity of cement ($\text{W}\cdot\text{m}^{-1}\cdot\text{K}^{-1}$)	1.03
Water depth (m)	90	Thermal conductivity of drilling fluid ($\text{W}\cdot\text{m}^{-1}\cdot\text{K}^{-1}$)	0.83
Lowering depth of casing (m)	5145	Thermal conductivity of casing ($\text{W}/\text{m}\cdot\text{K}$)	48.37
Kick off point (m)	4350	Density of formation ($\text{kg}\cdot\text{m}^{-3}$)	2241.7
Well diameter (mm)	212.725	Density of drilling fluid ($\text{kg}\cdot\text{m}^{-3}$)	2320
Outer diameter of casing (mm)	177.8	Density of cement slurry ($\text{kg}\cdot\text{m}^{-3}$)	2400
Inner diameter of casing (mm)	152.5	Specific heat capacity of drilling fluid ($\text{J}\cdot\text{kg}^{-1}\cdot\text{K}^{-1}$)	1600
Temperature at mud line ($^{\circ}\text{C}$)	10	Specific heat capacity of cement slurry ($\text{J}\cdot\text{kg}^{-1}\cdot\text{K}^{-1}$)	1840
Geothermal gradient ($^{\circ}\text{C } 100 \text{ m}^{-1}$)	4	Specific heat capacity of formation ($\text{J}\cdot\text{kg}^{-1}\cdot\text{K}^{-1}$)	840

Table 2. Basic parameters of Well X2.

Parameter	Value	Parameter	Value
Well type	Directional well	Thermal conductivity of formation ($\text{W}\cdot\text{m}^{-1}\cdot\text{K}^{-1}$)	2.03
Well depth (m)	5570	Thermal conductivity of cement ($\text{W}\cdot\text{m}^{-1}\cdot\text{K}^{-1}$)	1.03
Water depth (m)	90	Thermal conductivity of drilling fluid ($\text{W}\cdot\text{m}^{-1}\cdot\text{K}^{-1}$)	0.83
Lowering depth of casing (m)	5560	Thermal conductivity of casing ($\text{W}/\text{m}\cdot\text{K}$)	48.37
Kick off point (m)	4600	Density of formation ($\text{kg}\cdot\text{m}^{-3}$)	2241.7
Well diameter (mm)	212.725	Density of drilling fluid ($\text{kg}\cdot\text{m}^{-3}$)	2370
Outer diameter of casing (mm)	177.8	Density of cement slurry ($\text{kg}\cdot\text{m}^{-3}$)	2400
Inner diameter of casing (mm)	152.5	Specific heat capacity of drilling fluid ($\text{J}\cdot\text{kg}^{-1}\cdot\text{K}^{-1}$)	1610
Temperature at mud line ($^{\circ}\text{C}$)	10	Specific heat capacity of cement slurry ($\text{J}\cdot\text{kg}^{-1}\cdot\text{K}^{-1}$)	1840
Geothermal gradient ($^{\circ}\text{C } 100 \text{ m}^{-1}$)	4	Specific heat capacity of formation ($\text{J}\cdot\text{kg}^{-1}\cdot\text{K}^{-1}$)	840

The sensor was placed into well X1 to monitor the temperature of the cement slurry in real time. The monitoring values were compared with the results calculated by the temperature field model in this paper. The comparison result is shown in Figure 6. The comparison result (Figure 6) shows that, without considering the hydration reaction, the maximum error between the predicted results of the model and the monitored values reaches 21.6%. The maximum error between the predicted results and the monitored values is only 5.8% when hydration is taken into account. It shows that the influence of hydration reaction on the wellbore temperature field cannot be ignored, and the temperature field model established based on the hydration reaction can simulate the actual wellbore temperature well.

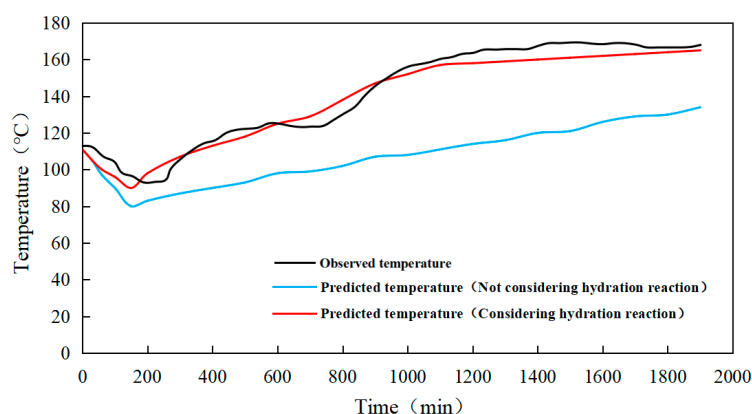


Figure 6. Comparison between the calculated temperature and the measured results.

The pressure loss of the cement slurry in the X1 well was monitored in real time by the sensor. The comparison result (Figure 7) between the predicted value calculated by the prediction model and the measured value shows that the pressure loss prediction model based on the hydration reaction dynamics of cement slurry can better simulate the actual pressure loss of cement slurry and meet the demand of anti-channeling.

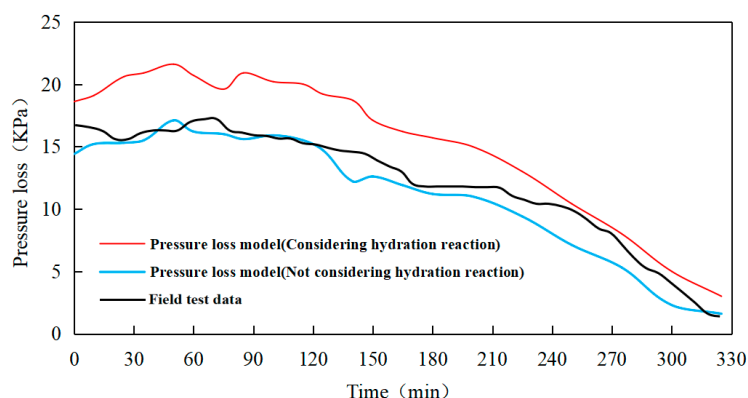


Figure 7. Comparison between the calculated pressure loss and the measured results.

Similarly, in the cementing process of Well X2, the sensors were attached to the outer wall of the casing at depths of 1470 m, 2500 m, 3720 m, 4540 m and 5318 m. Transient data of temperature and pressure at different depths were collected by different sensors in real time and compared with the calculated results of the model in this paper. As shown in Figures 8 and 9, the comparison results show that the trend of the predicted values and monitored values is basically consistent, and the maximum error is no more than 6%. The transient temperature and pressure calculated by this model can simulate the actual situation of the site well and better guide the evaluation of the anti-channeling performance of cement slurry and the optimization design of cement slurry systems.

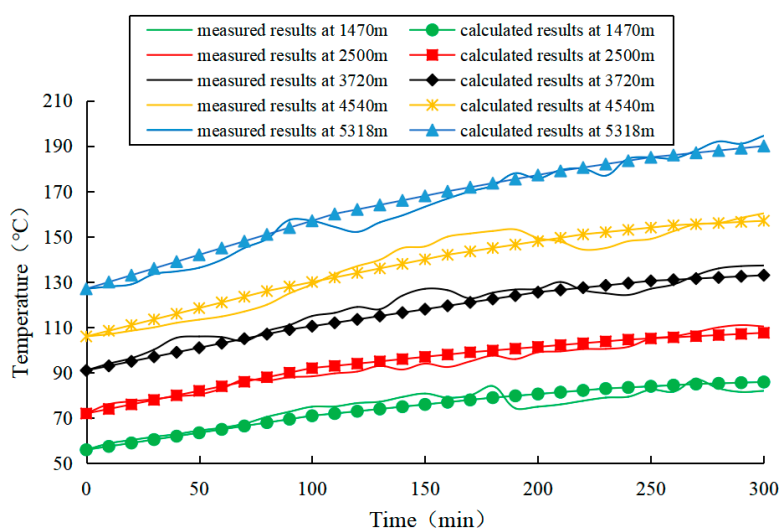


Figure 8. Comparison of calculated temperatures and measured temperatures.

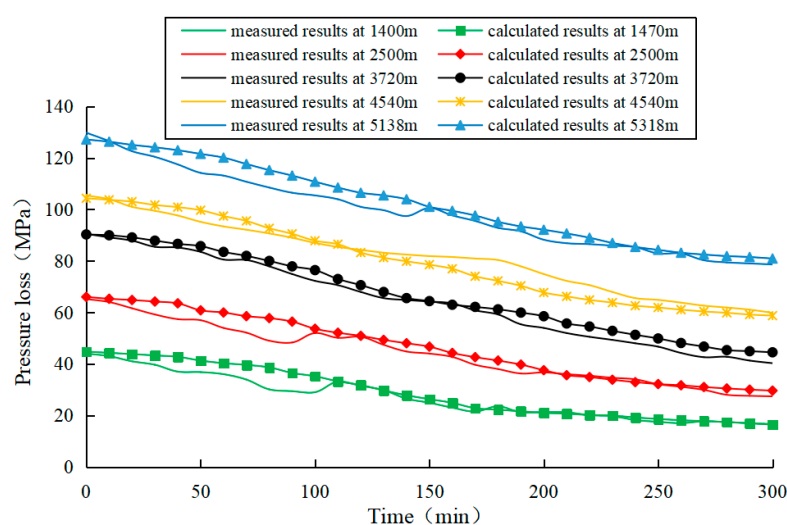


Figure 9. Comparison of calculated pressures and measured pressures.

5. Conclusions

A WOC pressure loss prediction model for HTHP wells is established according to the law of conservation of energy and the basic principles of hydrostatics. Then, coupled calculation of the temperature, pressure and hydration kinetic models is established by using the numerical difference method. The results obtained by iteration of the calculation process are conducive to the accurate prediction of the analytical solution of the wellbore temperature field, pressure field and pressure loss in the WOC stage, which ensures the convergence and stability of the model.

Under the action of the heat of hydration, the temperature of the cement slurry increases rapidly, leading to changes in the temperature field. Meanwhile, the change in the wellbore temperature field will react to the hydration reaction of the cement slurry and accelerate its hydration reaction rate. For HTHP wells, the properties of the large temperature difference will inevitably bring about temperature field changes.

As indicated in the results of the comparison between the predicted result and the measured result, the former fits the latter highly, with error controlled within 6%. Hence, this model can be well used to predict the pressure loss of HTHP wells and provide a basis for anti-channeling and pressure stabilization design in the WOC stage.

For the cementing operation of deep-water wells, it is necessary to consider that the low-temperature environment of the mud line and the heat release from the formation heat source will affect the waiting time of cement slurry, which may have an impact on the wellbore temperature field and the pressure loss the cement slurry. This is also the direction to be studied in the future.

Author Contributions: Conceptualization, X.L. and H.H.; methodology, K.L.; validation, Q.D., X.Z. and Y.T.; formal analysis, K.L.; investigation, H.H.; data curation, K.L.; writing—original draft preparation, K.L.; writing—review and editing, K.L. and H.H.; supervision, Q.D.; All authors have read and agreed to the published version of the manuscript.

Funding: This research received no external funding.

Institutional Review Board Statement: Not applicable.

Informed Consent Statement: Not applicable.

Data Availability Statement: The data presented in this study are available on request from the corresponding author. The data are not publicly available due to its storage in private networks.

Acknowledgments: The authors would like to thank the editor and reviewers for their sincere suggestions on improving the quality of this paper.

Conflicts of Interest: The authors declare no conflict of interest.

References

1. Ravi, K.; Biezen, E.N.; Lightford, S.C.; Hibbert, A.; Greaves, C. Deepwater cementing challenges. Paper SPE56534. In Proceedings of the SPE Annual Technical Conference and Exhibition, Houston, TX, USA, 26–29 September 1999.
2. Chen, W. Status and challenges of Chinese deepwater oil and gas development. *Petrol. Sci.* **2011**, *8*, 477–484. [\[CrossRef\]](#)
3. Christian, W.W.; Chatterji, J.; Ostroot, G.W. Gas leakage in primary cementing—a field study and laboratory investigation. *J. Petrol. Technol.* **1976**, *28*, 1361–1369. [\[CrossRef\]](#)
4. Wilkins, R.P.; Free, D. A new approach to the prediction of gas flow after cementing. In *SPE/IADC Drilling Conference*; Society of Petroleum Engineers: New Orleans, LA, USA, 1989.
5. Kremieniewski, M.; Wiśniowski, R.; Stryczek, S.; Orłowicz, G. Possibilities of Limiting Migration of Natural Gas in Boreholes in the Context of Laboratory Studies. *Energies* **2021**, *14*, 4251. [\[CrossRef\]](#)
6. Tao, C.; Rosenbaum, E.; Kutchko, B.G.; Massoudi, M. A Brief Review of Gas Migration in Oilwell Cement Slurries. *Energies* **2021**, *124*, 2369. [\[CrossRef\]](#)
7. API RP 10B-6. *Recommended Practice on Determining the Static Gel Strength of Cement Formulations*, 1st ed.; American Petroleum Institute (API): Washington, DC, USA, 2014.
8. Vazquez, G.; Blanco, A.M.; Colina, A.M. A Methodology to Evaluate the Gas Migration in Cement Slurries. In *SPE Latin American and Caribbean Petroleum Engineering Conference*; Society of Petroleum Engineers: Rio de Janeiro, Brazil, 2005.
9. Carter, G.; Slagle, K. A study of completion practices to minimize gas communication. *J. Petrol. Technol.* **1972**, *24*, 1170–1174. [\[CrossRef\]](#)
10. Sabins, F.L.; Tinsley, J.M.; Sutton, D.L. Transition time of cement slurries between the fluid and set states. *SPE J.* **1982**, *22*, 875–882. [\[CrossRef\]](#)
11. Sabins, F.L.; Sutton, D.L. The Relationship of Thickening Time, Gel Strength, and Compressive Strength of Oilwell Cements. *SPE Prod. Oper.* **1986**, *1*, 143–152. [\[CrossRef\]](#)
12. Drecq, P.; Parcevaux, P.A. A single technique solves gas migration problems across a wide range of conditions. In Proceedings of the International Meeting on Petroleum Engineering, Tianjin, China, 1–4 November 1988.
13. Sun, Z. The Relationship of Cement Slurry's Three Pore Pressure Drops due to Settling, Settling-Gelling and Hydrated Volume Shrinking-Gelling. *China Offshore Oil Gas.* **1999**, *11*, 51–54.
14. Zhang, X.; Guo, X.; Yang, Y. A Laboratorial Research on Estimating Channeling-Preventing Ability of Cement Slurry by Use of Gel Strength Method. *Nat. Gas. Ind.* **2001**, *21*, 52–55.
15. Zhang, X.; Liu, C.; Yang, Y. The important influence of cement slurry's stability on weight-loss. *J. Southwest Pet. Inst.* **2004**, *26*, 68–70.
16. Lin, F.; Meyer, C. Hydration kinetics modeling of Portland cement considering the effects of curing temperature and applied pressure. *Cem. Concr. Res.* **2009**, *39*, 255–265. [\[CrossRef\]](#)
17. Bu, Y.; Mu, H.; Jiang, L.; Liu, W.; Wei, X.; Wen, S. Modeling and laboratory studies of cement slurry weight loss. *Drill. Fluid Complet. Fluid* **2007**, *24*, 52–54.
18. Zhou, S.; Li, G.; Chu, Y. Sectional design for anti-gas channeling cementing. *Pet. Drill. Tech.* **2013**, *45*, 52–55.
19. Cheng, X.; Liu, K.; Li, Z.; Guo, X. Structure and properties of oil well cement slurry during liquid-solid transition. *Acta Pet. Sinica* **2016**, *37*, 1287–1292.
20. Liu, Y.; Chen, M.; Shi, F.; Li, Y.; Xian, M. Study and application of a technology for evaluating pressure loss of cement plug. *Drill. Flu Complet. Fluid* **2019**, *37*, 749–753.
21. Zhu, H.; Qu, J.; Liu, A.; Zou, J.; Xu, J. A New Method to Evaluate the Gas Migration for Cement Slurries. *Oilfield Chem.* **2012**, *29*, 353–356.
22. Li, Z.; Vandenbossche, J.M.; Iannacchione, A.T.; Brigham, J.C.; Kutchko, B.G. Theory-based review of limitations with static gel strength in cement/matrix characterization. *SPE Drill Complet.* **2016**, *31*, 145–158. [\[CrossRef\]](#)
23. Wooley, G.R. Computing downhole temperatures in circulation, injection, and production wells. *J. Petrol. Technol.* **1980**, *32*, 1509–1522. [\[CrossRef\]](#)
24. Cooke, C.E.; Kluck, M.P.; Medrano, R. Field measurements of annular pressure and temperature during primary cementing. *J. Petrol. Technol.* **1983**, *35*, 1429–1438. [\[CrossRef\]](#)
25. Krstulović, R.; Dabić, P. A conceptual model of the cement hydration process. *Cem. Concr. Res.* **2000**, *30*, 693–698. [\[CrossRef\]](#)
26. Moore, P.L. *Drilling Practice Manual*; Petroleum Publishing, Co.: Tulsa, OK, USA, 1974.
27. Wang, X.; Sun, B.; Liu, S.; Li, Z.; Liu, Z.; Wang, Z.; Li, H.; Gao, Y. A coupled model of temperature and pressure based on hydration kinetics during well cementing in deep water. *Petrol. Explor. Dev.* **2020**, *47*, 867–876. [\[CrossRef\]](#)
28. Pang, X.; Jimenez, W.C.; Iverson, B.J. Hydration kinetics modeling of the effect of curing temperature and pressure on the heat evolution of oil well cement. *Cem. Concr. Res.* **2013**, *54*, 69–76. [\[CrossRef\]](#)
29. Sun, B.; Wang, X.; Wang, Z.; Gao, Y. Transient temperature calculation method for deep-water cementing based on hydration kinetics model. *Appl. Therm. Eng.* **2018**, *129*, 1426–1434. [\[CrossRef\]](#)
30. Wang, X.; Wang, Z.; Deng, X.; Sun, B.; Zhao, Y.; Fu, W. Coupled thermal model of wellbore and permafrost in Arctic regions. *Appl. Therm. Eng.* **2017**, *123*, 1291–1299. [\[CrossRef\]](#)